

How to derive and compute 1,648 diagrams

Caleb C. Cannon and Andrei Derevianko

Department of Physics, University of Nevada, Reno, Nevada 89557

(Dated: November 21, 2018)

We present the first calculation for many-electron atoms complete through *fourth* order of many-body perturbation theory. Owing to an overwhelmingly large number of underlying diagrams, we developed a suite of symbolic algebra tools to automate derivation and coding. We augment all-order single-double excitation method with 1,648 omitted fourth-order diagrams and compute amplitudes of principal transitions in Na. The resulting *ab initio* relativistic electric-dipole amplitudes are in an excellent agreement with 0.05%-accurate experimental values. Analysis of previously unmanageable classes of diagrams provides a useful guide to a design of even more accurate, yet practical many-body methods.

PACS numbers: 31.15.Md, 31.15.Dv, 31.25.-v, 02.70.Wz

Many-body perturbation theory (MBPT) has proven to be a powerful tool in physics [1] and quantum chemistry [2]. Although MBPT provides a systematic approach to solving many-body quantum-mechanical problem, the number and complexity of analytical expressions and thus challenges of implementation grow rapidly with increasing order of MBPT (see Fig.1) Indeed, because of this complexity it has proven to be difficult to go beyond the complete third order in calculations for many-electron atoms (see, e.g., review [3]). At the same time, studies of higher orders are desirable for improving accuracy of *ab initio* atomic-structure methods. Such an improved accuracy is required, for example, in interpretation of atomic parity violation [4] and unfolding cosmological evolution of the fine-structure constant α [5].

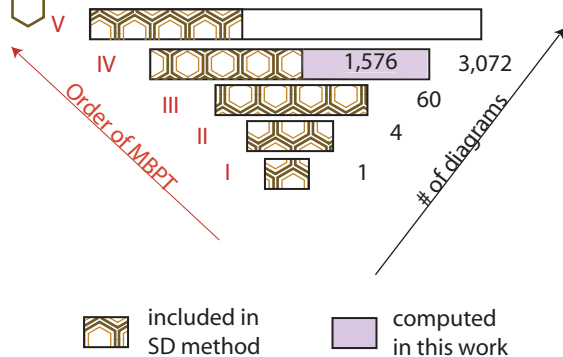


FIG. 1: Number of diagrams grows rapidly with the order of MBPT. Here we show number of topologically distinct Brueckner-Goldstone diagrams for transition amplitudes for univalent atoms. We assume that calculations are carried out in V^{N-1} Hartree-Fock basis to minimize the number of diagrams and we do not count “folded” [6] and normalization diagrams. All-order single-double (SD) excitations method recovers all diagrams through the third order, but misses roughly a half of diagrams in the fourth order. These 1,576 missed diagrams and 72 related normalization diagrams are explicitly computed in the present work.

Here we report the first calculation of transition amplitudes for alkali-metal atoms complete through the fourth

order of MBPT. We explicitly computed 1,648 topologically distinct Brueckner-Goldstone diagrams. To overcome such an overwhelming complexity we developed a symbolic problem-solving environment that automates highly repetitive but error-prone derivation and coding of many-body diagrams. Our work illuminates a crucial role of symbolic tools in problems unsurmountable in the traditional “pencil-and-paper” approach. Indeed, third-order calculation [7, 8] was a major research project most likely to have required a year to accomplish. As one progresses from the third to the present fourth order (see Fig. 1) there is a 50-fold increase in the number of diagrams. Simple scaling shows that present calculations require *half a century* to complete. With our tools derivation and coding take just a few minutes. Similar symbolic tools were developed by Perger et al. [9], however their package is so far limited to well-studied [7, 10] third order of MBPT. In contrast, we explore a wide range of new, previously unmanageable, classes of diagrams.

As an example of application of our symbolic technology, we compute electric-dipole amplitudes of the principal $3p_{3/2} - 3s_{1/2}$ and $3p_{1/2} - 3s_{1/2}$ transitions in Na. We augment all-order single-double excitations method [11] with 1,648 diagrams so that the formalism is complete through the fourth order (see Fig.1). The results are in excellent agreement with 0.05%-accurate experimental values [12]. Thus our computational method not only enables exploration of a wide range of previously unmanageable classes of diagrams but also defines new level of accuracy in *ab initio* relativistic atomic many-body calculations. Atomic units $|e| = \hbar = m_e = 4\pi\epsilon_0 \equiv 1$ are used throughout this paper.

Method— A practitioner of atomic MBPT typically follows these steps: (i) derivation of diagrams, (ii) angular reduction, and (iii) coding and numerical evaluation. Below we highlight components of our problem-solving environment designed to assist a theorist in these technically-involved tasks. First we briefly reiterate MBPT formalism [13] for atoms with a single valence electron outside a closed-shell core. For these systems a convenient point of departure is a single-particle basis generated in frozen-core (V^{N-1}) Dirac-Hartree-Fock (DHF) approxi-

mation [14]. In this approximation the number of MBPT diagrams is substantially reduced [6, 8]. The lowest-order valence wavefunction $|\Psi_v^{(0)}\rangle$ is simply a Slater determinant constructed from core orbitals and proper valence state v . The perturbation expansion is built in powers of residual interaction V_I defined as a difference between the full Coulomb interaction between the electrons and the DHF potential. The n^{th} -order correction to the valence wavefunction may be expressed as

$$|\Psi_v^{(n)}\rangle = -R_v \left\{ Q V_I |\Psi_v^{(n-1)}\rangle \right\}_{\text{linked}}, \quad (1)$$

where R_v is a resolvent operator modified to include so-called ‘‘folded’’ diagrams [13], projection operator $Q = 1 - |\Psi_v^{(0)}\rangle\langle\Psi_v^{(0)}|$, and only linked diagrams [6] are to be kept. From this recursion relation we may generate corrections to wave functions at any given order of perturbation theory. With such calculated corrections to wavefunctions of two valence states w and v , n^{th} -order contributions to matrix elements of an operator \hat{Z} are

$$Z_{wv}^{(n)} = \sum_{k=0}^{n-1} \langle\Psi_w^{(n-k-1)}|Z|\Psi_v^{(k)}\rangle_{\text{val, conn}} + Z_{wv, \text{norm}}^{(n)}. \quad (2)$$

Here $Z_{wv, \text{norm}}^{(n)}$ is a normalization correction arising due to an intermediate normalization scheme employed in derivation of Eq. (1). Subscript ‘‘val, conn’’ indicates that only connected diagrams involving excitations from valence orbitals are included in the expansion.

Equations (1) and (2) completely define a set of many-body diagrams at any given order of MBPT. In practice the derivations are carried out in the second quantization and the Wick’s theorem [6] is used to simplify products of creation and annihilation operators. Although the application of the Wick’s theorem is straightforward, as order of MBPT increases, the sheer length of expressions and number of operations becomes quickly unmanageable. We developed a symbolic-algebra package written in *Mathematica* [15] to carry out this task. The employed algorithm relies on decision trees and pattern matching, i.e., programming elements typical to artificial intelligence applications. With the developed package we fully derived fourth-order corrections to matrix elements of univalent systems [13].

This is one of the fourth-order terms from Ref. [13]

$$\sum_{abc\ mnr} \frac{z_{bv} \tilde{g}_{canr} g_{nr cm} \tilde{g}_{mwab}}{(\varepsilon_w - \varepsilon_b)(\varepsilon_{mw} - \varepsilon_{ab})(\varepsilon_{nrw} - \varepsilon_{abc})}. \quad (3)$$

There are 524 such contributions in the fourth order [16]. Here abbreviation $\varepsilon_{xy\dots z}$ stands for $\varepsilon_x + \varepsilon_y + \dots + \varepsilon_z$, with ε_x being single-particle DHF energies. Further, g_{ijkl} are matrix elements of electron-electron interaction in the basis of DHF orbitals. The quantities \tilde{g}_{ijkl} are antisymmetric combinations $\tilde{g}_{ijkl} = g_{ijlk} - g_{ijkl}$. The summation is over single-particle DHF states. Core orbitals are enumerated by letters a, b, c and complementary excited states are labelled by m, n, r . Finally matrix elements of the operator \hat{Z} in the DHF basis are denoted as z_{ij} .

The summations over magnetic quantum numbers are usually carried out analytically. This ‘‘angular reduction’’ is the next major technically-involved step. We also automate this task. The details are provided in Ref. [17]. Briefly, the angular reduction is based on application of the Wigner-Eckart (WE) theorem [18] to matrix elements z_{ij} and g_{ijkl} . The WE theorem allows one to ‘‘peel off’’ dependence of the matrix elements on magnetic quantum numbers in the form of 3j-symbols and reduced matrix elements. In the particular case of fourth-order terms, such as Eq. (3), application of the WE theorem results in a product of seven 3j-symbols. To automate simplification of the products of 3j-symbols we employed a symbolic program *Kentaro* developed by Takada [19].

The result of angular reduction of our sample term (3) is

$$\sum_{abc mnr} \sum_L \frac{\delta_{ja jm} \delta_{jb jw} (-1)^{j_a + j_c + j_n + j_r}}{(2L+1) \sqrt{(2j_a+1)(2j_w+1)}} \frac{\langle b||z||v\rangle Z_L(\text{canr}) X_L(\text{nrcm}) Z_0(\text{mwab})}{(\varepsilon_w - \varepsilon_b)(\varepsilon_{mw} - \varepsilon_{ab})(\varepsilon_{nrw} - \varepsilon_{abc})}.$$

Here the reduced quantities $\langle i||z||j\rangle$, $X_L(ijkl)$, and $Z_L(ijkl)$ depend only on total angular momenta and principal quantum numbers of single-particle orbitals.

As a result of angular reduction we generate analytical expressions suitable for coding. We also automated the tedious coding process by developing custom parsers based on Perl and Mathematica. These parsers translate analytical expressions into Fortran90 code. The resulting code is very large - it is about 20,000 lines long and were it be programmed manually, it would have required several years to develop. For numerical evaluation we employed a B-spline library[20]. All the fourth-order results were computed with a sufficiently large basis of 25 out of 30 lowest-energy ($E > mc^2$) spline functions for each partial wave through $h_{11/2}$.

At this point we have demonstrated feasibility of working with thousands of diagrams in atomic MBPT. Now we apply our computational technique to high-accuracy calculation of transition amplitudes in Na.

Fourth-order diagrams complementary to single-double excitations method. One of the mainstays of practical applications of MBPT is an assumption of convergence of series in powers of the perturbing interaction. Sometimes the convergence is poor and then one sums certain classes of diagrams to ‘‘all orders’’ using iterative techniques. In fact, the most accurate many-body calculations of parity violation in Cs by Dzuba et al. [21] and Blundell et al. [22] are of this kind. These techniques, although summing certain classes of MBPT diagrams to all orders, still do not account for an infinite number of residual diagrams (see Fig. 1). In Ref. [13] we proposed to augment a given all-order technique with some of the omitted diagrams so that the formalism is complete through a certain order of MBPT. As in that work, here we consider an improvement of all-order single-double (SD) excitation method employed in Ref. [22]. Here a certain level n

of excitations from lowest-order wavefunction refers to an all-order grouping of contributions in which n core and valence electrons are promoted to excited single-particle orbitals. The SD method is a simplified version of the coupled-cluster expansion truncated at single and double excitations.

The next step in improving the SD method would be an inclusion of triple excitations. However, considering present state of available computational power, the complete incorporation of triples seems as yet impractical for heavy atoms. Here we investigate an alternative illustrated in Fig. 1 : we compute the dominant contribution of triples in a direct fourth-order MBPT for transition amplitudes. We also account for contribution of disconnected quadruple excitations in the fourth order. In Ref. [13], we separated these complementary diagrams into three major categories by noting that triples and disconnected quadruples enter the fourth order matrix element $Z_{wv}^{(4)}$ via (i) an *indirect* effect of triples and disconnected quadruples on single and double excitations in the third-order wavefunction — we denote this class as $Z_{0\times 3}$; (ii) *direct* contribution to matrix elements labelled as $Z_{1\times 2}$; (iii) correction to normalization denoted as Z_{norm} . Further these categories were broken into subclasses based on the nature of triples, so that

$$\begin{aligned} \left(Z_{wv}^{(4)}\right)_{\text{non-SD}} &= Z_{1\times 2}(T_v) + Z_{1\times 2}(T_c) + \\ &Z_{0\times 3}(S_v[T_v]) + Z_{0\times 3}(D_v[T_v]) + \\ &Z_{0\times 3}(S_c[T_c]) + Z_{0\times 3}(D_v[T_c]) + \\ &Z_{1\times 2}(D_{nl}) + Z_{0\times 3}(D_{nl}) + Z_{\text{norm}}(T_v). \end{aligned} \quad (4)$$

Here we distinguished between valence (T_v) and core (T_c) triples and introduced a similar notation for singles (S) and doubles (D). Notation like $S_v[T_c]$ stands for effect of second-order core triples (T_c) on third-order valence singles S_v . Diagrams D_{nl} are contributions of disconnected quadruples (non-linear contributions from double excitations). The reader is referred to Ref. [13] for further details and discussion.

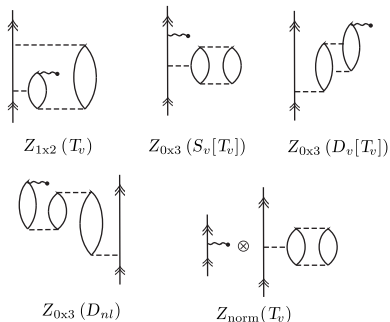


FIG. 2: Representative fourth-order diagrams involving triple and disconnected quadruple excitations.

Transition amplitudes in Na. Using our problem-solving environment we derived the 1,648 complementary diagrams [13], carried out angular reduction [17],

and generated Fortran 90 code suitable for any univalent system. As an example we evaluate reduced electric-dipole matrix elements of $3s_{1/2} - 3p_{1/2,3/2}$ transitions in Na (eleven electrons)[23]. Our numerical results are presented in Table I. Analyzing this table we see that leading contributions come from valence triples T_v . Similar conclusion can be drawn from our preliminary calculations for heavier Cs atom. Dominance of valence triples (T_v) over core triples (T_c) may be explained by smaller energy denominators for T_v terms. Representative diagrams for these relatively large contributions are shown in Fig. 2. Based on this observation we propose to fully incorporate valence triples into a hierarchy of coupled-cluster equations and add a perturbative contributions of core triples. Such an all-order scheme would be a more accurate and yet practical extension of the present calculations.

Another point we would like to discuss is a sensitivity of our results to higher-order corrections. In Table I, all large contributions add up coherently, possibly indicating a good convergence pattern of MBPT. However, we found large, factor of 100, cancellations of terms inside the $Z_{0\times 3}(S_v[T_v])$ class. In principle higher-order MBPT corrections may offset a balance between cancelling terms and an all-order treatment is desired. Fortunately, the $Z_{0\times 3}(S_v[T_v])$ class of diagrams (combined with parts of $Z_{1\times 2}(T_v)$) have been taken into account in all-order SDpT (SD + partial triples) method [22, 24]. We correct our results for the difference between all-order [25] and our fourth-order values for these diagrams (last row of Table I). These all-order corrections modify our final values of complementary diagrams by 15%.

Class	Number of diagrams	$3p_{1/2} - 3s_{1/2}$	$3p_{3/2} - 3s_{1/2}$
Connected triples			
$Z_{0\times 3}(S_v[T_v])$	72	-0.8[-3]	-1.1[-3]
$Z_{0\times 3}(D_v[T_v])$	432	-2.2[-3]	-3.0[-3]
$Z_{1\times 2}(T_v)$	504	-0.7[-3]	-1.0[-3]
$Z_{\text{norm}}(T_v)$	72	-0.7[-3]	-1.2[-3]
$Z_{0\times 3}(D_v[T_c])$	144	-0.01[-3]	-0.01[-3]
$Z_{0\times 3}(S_c[T_c])$	72	0.06[-3]	0.09[-3]
$Z_{1\times 2}(T_c)$	216	0.03[-3]	0.04[-3]
Total triples	1512	-4.3[-3]	-6.3[-3]
Disconnected quadruples			
$Z_{0\times 3}(D_{nl})$	68	1.1[-3]	1.6[-3]
$Z_{1\times 2}(D_{nl})$	68	0.2[-3]	0.3[-3]
Total quads	136	1.4[-3]	2.0[-3]
Total	1648	-2.6[-3]	-4.3[-3]
+ $\delta(\text{SDpT})$		-3.3[-3]	-4.9[-3]

TABLE I: Fourth-order complementary contributions to reduced electric-dipole matrix elements $\langle 3p_j || D || 3s_{1/2} \rangle$ in Na. Last row marked “+ $\delta(\text{SDpT})$ ” is the total value corrected using all-order SDpT values as discussed in the text. Notation $x[y]$ stands for $x \times 10^y$.

In Table II we add our complementary diagrams to

SD matrix elements [11] and compare with experimental values. Several high-accuracy experiments have been carried out for Na, resolving an apparent disagreement between an earlier measurement and calculated lifetimes [see review 26, and references therein]. In Table II we compare with the results of the two most accurate experiments [12, 27]. The SD method [11] overestimates these experimental values by 2.5σ and 2.8σ respectively (σ is experimental uncertainty). With our fourth-order corrections taken into consideration the comparison significantly improves. The resulting *ab initio* matrix elements for both $3p_{1/2} - 3s_{1/2}$ and $3p_{3/2} - 3s_{1/2}$ transitions are in an excellent agreement with 0.05%-accurate values from Ref. [12] and differ by 1.2σ from less-accurate results of Ref. [27]. Considering this agreement it would be desirable to have experimental data accurate to 0.01%.

	$3p_{1/2} - 3s_{1/2}$	$3p_{3/2} - 3s_{1/2}$
Singles-doubles [28]	3.5307	4.9930
$(Z^{(4)})_{\text{non-SD}}$	-0.0033	-0.0049
Total	3.5274	4.9881
	Experiment	
Jones et al. [12]	3.5267(17)	4.9875(24)
Volz et al. [27]	3.5246(23)	4.9839(34)

TABLE II: Comparison of the calculated reduced electric-dipole matrix element $\langle 3p_j || D || 3s_{1/2} \rangle$ of principal transitions in Na with experimental data.

We demonstrated that symbolic tools can replace multi-year detailed development efforts in atomic MBPT with an interactive work at a conceptual level, thus enabling an exploration of ever more sophisticated techniques. As an example, we presented the first calculations for many-electron atoms complete through fourth order, a task otherwise requiring half a century to complete. Although even at this level the computed transition amplitudes for Na indicate a record-setting *ab initio* accuracy of a few 0.01%, the calculations allowed us to gain insights into relative importance of various contributions and to propose even more accurate yet practical many-body method. With an all-order generalization [13] of the derived diagrams we plan to address a long-standing problem [21, 22] of improving theoretical accuracy of interpretation of parity violation in Cs atom [29].

We would like to thank W.R. Johnson, V.A. Dzuba, W.F. Perger, and K. Takada for useful discussions and M.S. Safronova for providing detailed breakdown of SDpT and SD results. This work was supported in part by the National Science Foundation.

-
- [1] A. L. Fetter and J. D. Walecka, *Quantum Theory of Many-particle Systems* (McGraw-Hill, 1971).
- [2] A. Szabo and N. S. Ostlund, *Modern Quantum Chemistry* (Macmillan, New York, 1982).
- [3] J. Sapirstein, Rev. Mod. Phys. **70**, 55 (1998).
- [4] I. B. Khriplovich, *Parity Nonconservation in Atomic Phenomena* (Gordon & Breach, Philadelphia, 1991); M.-A. Bouchiat and C. Bouchiat, Rep. Prog. Phys. **60**, 1351 (1997).
- [5] J. K. Webb, M. T. Murphy, V. V. Flambaum, V. A. Dzuba, J. D. Barrow, C. W. Churchill, J. X. Prochaska, and A. M. Wolfe, Phys. Rev. Lett. **87**, 091301 (2001).
- [6] I. Lindgren and J. Morrison, *Atomic Many-Body Theory* (Springer-Verlag, Berlin, 1986), 2nd ed.
- [7] W. R. Johnson, Z. W. Liu, and J. Sapirstein, At. Data Nucl. Data Tables **64**, 279 (1996).
- [8] S. A. Blundell, D. S. Guo, W. R. Johnson, and J. Sapirstein, At. Data Nucl. Data Tables **37**, 103 (1987).
- [9] W. F. Perger, M. Xia, K. Flurchick, and M. I. Bhatti, Comp. Sci. Eng. **3**, 38 (2001).
- [10] S. A. Blundell, W. R. Johnson, and J. Sapirstein, Phys. Rev. A **42**, 3751 (1990).
- [11] M. S. Safronova, A. Derevianko, and W. R. Johnson, Phys. Rev. A **58**, 1016 (1998).
- [12] K. M. Jones, P. S. Julienne, P. D. Lett, W. D. Phillips, E. Tiesinga, and C. J. Williams, Europhys. Lett. **35**, 85 (1996).
- [13] A. Derevianko and E. D. Emmons, Phys. Rev. A **65**, 052115 (2002).
- [14] H. P. Kelly, Adv. Chem. Phys. **14**, 129 (1969).
- [15] S. Wolfram, *The Mathematica Book* (Wolfram Media/Cambridge University Press, Champaign, Illinois, 1999), 4th ed.
- [16] This number does not include folded diagrams or normalization correction. In contrast to Ref. [13] we have also counted so-called Hermitian conjugated terms as a separate contribution. When anisymmetrized Coulomb matrix elements \tilde{g}_{ijkl} are expanded, term (3) is represented by four topologically unique Brueckner-Goldstone diagrams.
- [17] A. Derevianko, e-print:physics/0212008.
- [18] A. R. Edmonds, *Angular Momentum in Quantum Mechanics* (Princeton University Press, 1985).
- [19] K. Takada, Comp. Phys. Comm. **69**, 142 (1992).
- [20] W. R. Johnson, S. A. Blundell, and J. Sapirstein, Phys. Rev. A **37**, 307 (1988).
- [21] V. A. Dzuba, V. V. Flambaum, and O. P. Sushkov, Phys. Lett. A **141**, 147 (1989).
- [22] S. A. Blundell, W. R. Johnson, and J. Sapirstein, Phys. Rev. Lett. **65**, 1411 (1990), Phys. Rev. D **45**, 1602 (1992).
- [23] Several high-accuracy experimental data sets are available for these transitions and, unlike hyperfine-structure constants, an interpretation is free from QED and nuclear structure uncertainties.
- [24] M. S. Safronova, W. R. Johnson, and A. Derevianko, Phys. Rev. A **60**, 4476 (1999).

- [25] M. S. Safronova (private communications).
- [26] U. Volz and H. Schmoranzer, Phys. Scr. **T65**, 48 (1996).
- [27] U. Volz, M. Majerus, H. Liebel, A. Schmitt, and H. Schmoranzer, Phys. Rev. Lett. **76**, 2862 (1996).
- [28] We recomputed SD values to more significant digits compared to Ref. [11].
- [29] C. S. Wood, S. C. Bennett, D. Cho, B. P. Masterson, J. L. Roberts, C. E. Tanner, and C. E. Wieman, Science **275**, 1759 (1997).